J. Chem. Chem. Eng. 6 (2012) 526-530

Synthesis and Structural Characterization of Sm-Sr Nickelates

Patrícia Mendonça Pimentel[1], Rosane Maria Pessoa Betânio Oliveira[1, 2*], José Humberto Araújo[3], Filipe Silva Oliveira[1], Osmar Roberto Bagnato[4] and Dulce Maria de Araújo Melo[1]

1. Catalysis and Materials Laboratory, Federal University of Rio Grande do Norte, Natal, RN, 59078-970, Brazil

2. Faculty of Materials Engineering, Federal University of Pará, Marabá, PA, 68505-080, Brazil

3. International Institute of Physics, Federal University of Rio Grande do Norte, Natal, RN, 59078-970, Brazil

4. Brazilian Synchrotron Light Laboratory, Campinas, SP, 13083-970, Brazil

Received: April 15, 2012 / Accepted: May 08, 2012 / Published: June 25, 2012.

Abstract: The main purpose of this work was to obtain Sm-Sr nickelates nanoparticles with Ruddelsden-Popper type structures obtained by a simple process such as gelatin synthesis. The powders were calcinated at 900 ºC and characterized by X-ray diffraction, thermogravimetric analysis, scanning electron microscopy and high-resolution transmission electron microscopy techniques. The effect of chemical substitution of the Sm^{3+} by Sr^{2+} ions on the structural properties of the powders was studied. The Rietveld's method was successfully applied for determination of the quantitative phase analysis of the powders and revealed that the main phase of the powders for different strontium content is of Ruddelsden-Popper type structure. A symmetry change from orthorhombic to tetragonal is observed as increasing strontium.

Key words: Nanostructures, electron microscopy, X-ray diffraction, Ruddelsden-Popper.

1. Introduction

The RP (Ruddlesden Popper) compounds with general formula of $A_{n+1}B_nO_{3n+1}$ consist of $n(ABO_3)$ perovskite blocks, separated by a rock salt-like layer of composition AO, where n represents the number of connected layers of vertex sharing BO_6 octahedra [1]. These oxides constitute one of the most important families of layered perovskites owing to various properties of technological interest. In particular, the nickel and lanthanide ions containing RP-phases have received considerable attention, because of their remarkable electrical, magnetic, and catalytic properties [2-6]. Recently, studies showed that $La_{n+1}Ni_nO_{3n+1}$ and $Sm_{2-x}Sr_xNiO_4$ RP-type exhibited interesting properties for use as cathode materials of IT-SOFC (intermediate temperature solid oxide fuel cells) [7, 8].

Most of techniques be used to obtain of RP-phases need high temperatures, oxygen flow and extended calcination periods [5, 9, 10]. In this work, oxides belonging to the $Sm_{2-x}Sr_xNiO_4$ (x = 0.4, 0.8 and 1.2) systems were synthesized by a gelatin-based gel route, in order to evaluate the evolution of structural properties of these oxides with increasing content of strontium. The synthesis by using gelatin provides an interesting alternative to other elaborate techniques because it offers several attractive advantages such as: simplicity of experimental setup and short time between the preparation of reactants and the availability of the final product. In addition, there have been only a few reports on the synthesis and the characterization of this system.

*Corresponding author: Rosane Maria Pessoa Betânio Oliveira, Prof./Dsc., research field: materials chemistry. E-mail: rosaneboliveira@gmail.com.

2. Experiment

2.1 Synthesis

Four samples of strontium and samarium nickelates were synthesized by using gelatin powder (GELITA®) as organic precursor and metallic nitrates as starting materials. The samples were named A, B, C and D for samarium replacement by strontium in amount correspondent to 20%, 40%, 60% and 80%, respectively. In the synthesis procedure, the gelatin was added to a beacker containing deionized water under stirring for 30 minutes at 50 ºC. $Ni(NO_3)_2{\cdot}6H_2O$ (99.9%-SIGMA-ALDRICH) and $Sm(NO_3){\cdot}6H_2O$ (99.9%-SIGMA-ALDRICH) were added to the solution at 70 °C for some minutes. The temperature was slowly increased up to 90 °C and the solution was stirred on a hot plate until it became a gel. This gel was calcined at 350 ºC for 2 h with a heating rate at 5 °Cmin^{-1}, resulting in a precursor powder. The powder was calcined at 900 °C for 4 h and characterized for several techniques.

2.2 Characterization

Thermogravimetric curves were recorded using a Shimadzu TGA/DTA-60H thermal analyzer under air atmosphere. Temperature range was between 25 °C and 800 °C with a heating rate of 5 °C.min^{-1}. The X-ray patterns were obtained from samples calcined at different temperatures. Measurements were recorded on a Shimadzu XRD-6000 diffractometer with monochromatic radiation of CuKα1 (λ = 1.5406 Å). A 2θ angular range was used between 10° and 90° with a scan rate of 2°min^{-1} and step of 0.02°. Crystalline phases were identified using the ICDD (international center for diffraction data) database. The Rietveld method was used to refine the XRD data using the MAUD program (version 2.044). The FEG-SEM (field emission gun scanning electron microscopy) images of the powders were examined in a JEOL JSM 6330F microscope. HRTEM (high-resolution transmission electron microscopy) images were obtained with a HRTEM JEM 3010 URP electron microscope. The specific surface areas were measured by nitrogen adsorption on NOVA2000 BET system.

3. Results and Discussion

Thermogravimetric curves of the gelatin (a) and precursor powders (b-e) are shown in Fig. 1. In the temperature region between 30 ^oC and 900 ^oC the TG curves of all samples show a decrease in sample weight associated with the loss of water and gelatin decomposition. The (a) curve indicates that gelatin decomposition occurs in three distinct stages. In the first stage, a reduction of 12% is related to moisture (water of hydration). In the second stage, approximately 45% is due to the elimination of aminoacid fragments, usually proline, which is thermodynamically susceptible to thermal degradation in an oxidant atmosphere [11]. A loss of around 43% in the final stage can be attributed to glycine degradation. The precursor powders curves (b-e) are similar and the complete decomposition of the gelatin occurs at higher temperatures. This is due to the interaction of glycine through carboxyl groups and amine with metallic ions. Then, chelates are formed, giving more structural stability and avoiding oxidation of the high glycine content [11]. Loss of mass in these powders varied from 6.9% to 35%.

Fig. 2 shows the observed and calculated X-ray powder patterns of crystallization products containing the Sm-Sr nickelates solid solutions with varying

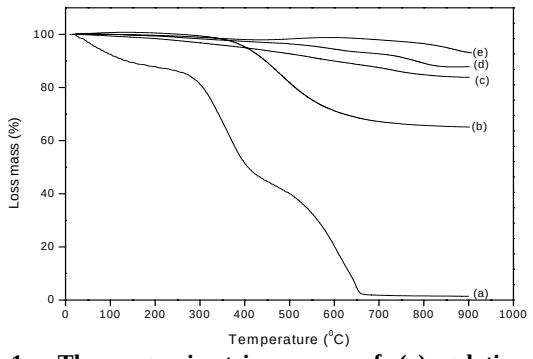

Fig. 1 Thermogravimetric curves of (a) gelatin and precursors powders of samples (b) A, (c) B, (d) C and (e) D.

strontium content. The quantitative analysis of samples and crystallite size obtained by MAUD program is given in Table 1. The GoF (goodness of fitting) values of all the fitted patterns lie between 1.18-1.34. The average crystallite sizes ranged from 34 nm to 40 nm. The unit-cell parameters for RP phase were determined with precision from the results of Rietveld refinements and are shown in Table 2. The results show that oxides with 20% and 40% Sr have an orthorhombic symmetry (Fmmm space group) and a tetragonal symmetry (I4/mmm space group) with substitution of 60% and 80%. It was reported that the substitution of Nd by Sr in Nd_2NiO_4 might induce a structural phases transition from orthorhombic to tetragonal symmetry leading to a mixed valence (Ni^{2+}/Ni^{3}) for the transition metal ion, which would in turn induce interesting electrical and magnetic properties in this system [6]. It is observed that the tetragonal $Sm_{0.8}Sr_{1.2}NiO_4$ structure-type can be preserved when the substitution of Sm^{3+} for Sr^{2+} amounts up to 60% of strontium content. Then, it can be concluded that the upper limit for the substitution

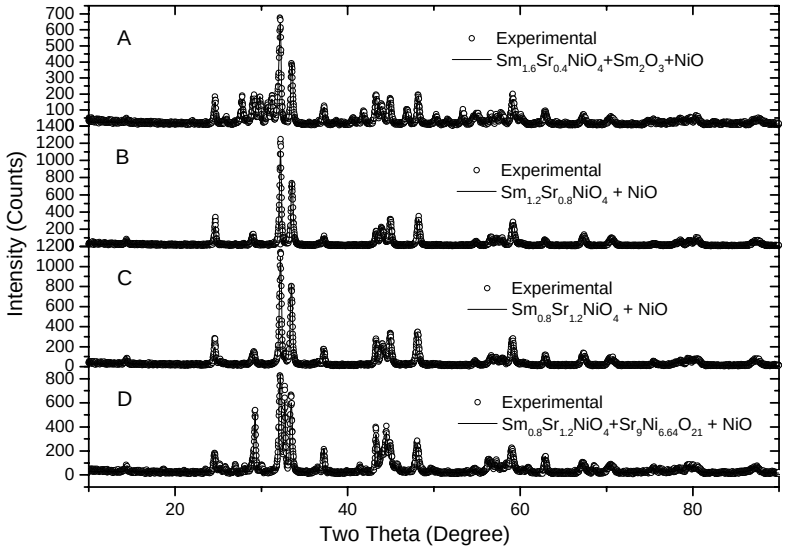

Fig. 2 The evolution of the X-rays diffractograms as a function of Sr content.

Table 1 Quantitative analysis of samples and crystallite size obtained by MAUD refinement.

Sample	Crystallite size (nm)	Phases (%)	
A	37.53	$Sm_{1.6}Sr_{0.4}NiO_4$	47.73
		Sm_3O_2	33.74
		NiO	18.53
B	40.94	$Sm_{1.2}Sr_{0.8}NiO_4$	87.75
		NiO	12.25
C	36.19	$Sm_{0.8}Sr_{1.2}NiO_4$	85.88
		NiO	14.12
D	34.57	$Sm_{0.8}Sr_{1.2}NiO_4$	51.51
		$Sr_9Ni_{6.64}O_{21}$	34.32
		NiO	14.16

Table 2 Lattice parameters for RP phase according to Rietveld refinement.

Sample	RP phase	Symmetry	Space group	Lattice parameters		
				a	*b*	*c*
A	$Sm_{1.6}Sr_{0.4}NiO_4$	orthorhombic	Fmmm	5.3299	5.3465	12.3041
B	$Sm_{1.2}Sr_{0.8}NiO_4$	orthorhombic	Fmmm	5.3273	5.3431	12.2922
C	$Sm_{0.8}Sr_{1.2}NiO_4$	tetragonal	I4/mmm	3.7804	3.7804	12.2613
D	$Sm_{0.8}Sr_{1.2}NiO_4$	tetragonal	I4/mmm	3.7850	3.7850	12.2859

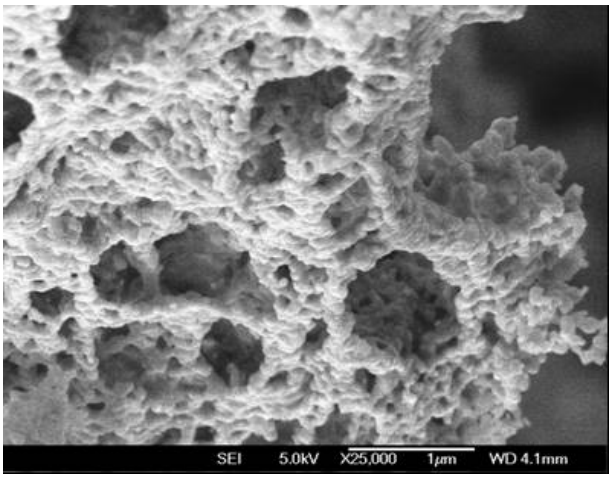

Fig. 3 FEG-SEM image of sample C.

of Sr in RP phase was 60%, once in higher value resulted in strontium segregation and formation of significant amount of $Sr_9Ni_{6.64}O_{21}$ phase. This compound is member (n = 2) of the Perovskite-Related A3n+3A'n B3+nO9+6n family and the structure is the result of stacking infinite layers perpendicular to the c axis in the sequence one $[Sr_3O_9]$ layer plus two $[Sr_3NiO_6]$ layers [12]. Nevertheless, it is observed a significant amount of Sm_2O_3 for lower substitution of Sr in RP phase. Small amount of NiO was detected in all samples.

FEG-SEM image is shown in Fig. 3. As can be seen,

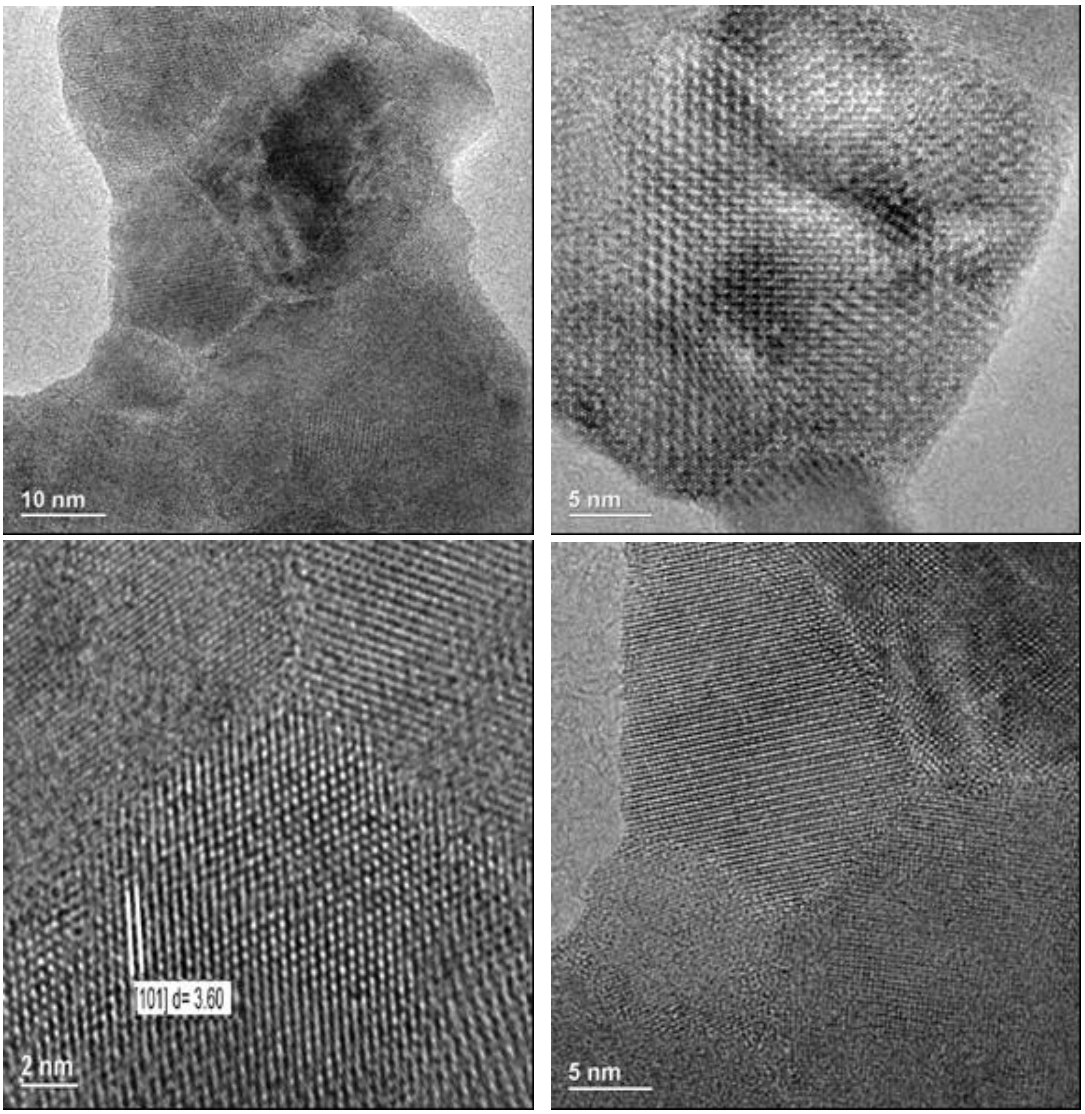

Fig. 4 HRTEM images of sample C.

the powder obtained by gelatin is constituted by rounded agglomerates of crystalline nanosized particles. The porous surface of the material is caused by the evolution of high gas content during synthesis and powder production. The gelatin provides to the system a large amount of organic matter, which is removed during calcination and favors the appearance of pores in the material. The specific surface area of the powders range from 11 to 23 m^2/g. These area values are relatively high for perovskite type oxides and can be a consequence of high porosity of the powders. The morphology of the powders was also investigated by HRTEM analysis, as shown in Fig. 4. It is observed that the powder is composed of many particles agglomerate with average grain size higher than 10 nm. The images show clearly the regular crystal lattice distance which expresses the high crystalline of compound formed. The higher-magnification image of the particles confirms that a region of a single grain consists of nearly equally spaced lattice rows where we can see the Rec. [101] planes with $d = 3.60$ Å.

4. Conclusions

The present study shows that the gelatin route provides a simple means of preparing oxides with Ruddlesden-Popper structure at low temperatures and pression conditions. Besides its low cost, this method can be applied on large scale preparations due to its simplicity. The samples were not single phase, but the results of phase analysis show that Ruddelsden-Popper is a dominant phase in all crystallization products. Refinement process shows that $Sm_{2-x}Sr_xNiO_4$ possesses orthorhombic symmetry and exhibits a phase transition to tetragonal symmetry upon Sr^{2+} content (> 40%). SEM-FEG image revealed that the powders are nanosized and highly porous.

Acknowledgments

The authors are grateful to CNPq for the financial support, GELITA for supplying the gelatin, and LNLS (National Synchrotron Light Laboratory) for SEM and TEM images.

References

[1] Greenblatt, M. Curr. Ruddlesden-Popper $Ln_{n+1}Ni_nO_{3n+1}$ Nickelates: Structure and Properties. *Current Opinion in Solid State & Materials Science* **1997,** *2,* 174-183.

[2] Zhang, Z.; Greenblatt, M. Synthesis, Structure and Properties of (Ln = La, Pr, and Nd). *Journal of Solid State Chemistry* **1995,** *117,* 236-246.

[3] Wu, G.; Neumeier, J. J.; Hundley, M. F. Magnetic Susceptibility, Heat Capacity, and Pressure Dependence of the Electrical Resistivity of $La_3Ni_2O_7$ and $La_4Ni_3O_{10}$. *Physical Review B* **2001,** *63,* 245-249.

[4] Jurado, J. R. Present Several Items on Ceria-Based Ceramic Electrolytes: Synthesis Additive Effects, Reactivity and Rlectrochemical Behavior. *Journal of Materials Science* **2001,** *36,* 1133-1139.

[5] Mogni, L.; Prado, F.; Ascolani, H.; Abbate, M.; Moreno, M. S.; Manthiram, A.; et al. Synthesis, Crystal Chemistry and Physical Properties of The Ruddlesden-Popper Phases $Sr_3Fe_{2-x}Ni_xO_{7-\delta}$ ($0 \le x \le 1.0$). *Journal of Solid State Chemistry* **2005,** *178,* 1559-1568.

[6] Arbuckle, B. W.; Ramanujachary, K. V.; Zhang, Z.; Greenblatt, M. Investigations on the Structural, Electrical, and Magnetic Properties of $Nd_{2-x}Sr_xNiO_{4+\delta}$. *Journal Solid State Chemistry* **1990,** *88,* 278-290.

[7] Qiang, L.; Yong, F.; Hui, Z.; Li-Ping, S.; Li-Hua, H. Preparation and Electrochemical Properties of a $Sm_{2-x}Sr_xNiO_4$ Cathode for an IT-SOFC**.** *Journal of Power Sources* **2007,** *167,* 64-68.

[8] Amow, G.; Davidson, I. J.; Skinner, S. J. A Comparative Study of the Ruddlesden-Popper Series, $La_{n+1}Ni_nO_{3n+1}$ (*n* = 1, 2 and 3), for Solid-Oxide Fuel-Cell Cathode Applications. *Solid State Ionics* **2006,** *177,* 1205-1210.

[9] Napierala, C.; Lepoittevin, C.; Edely, M.; Sauques, L.; Giovanelli, F.; Laffez, P.; et al. Moderate Pressure Synthesis of Rare Earth Nickelate with Metal-Insulator Transition Using Polymeric Precursors. *Journal Solid State Chemistry* **2010,** *183,* 1663-1669.

[10] Chaker, H.; Roisnel, T.; Potel, M.; Hassen, R. B. Structural and Electrical Changes in $NdSrNiO_{4-\delta}$ by Substitute Nickel with Copper. *Journal of Solid State Chemistry* **2004,** *177,* 4067-4072.

[11] De Menezes, A. S.; Remédios, C. M. R.; Sasaki, J. M.; Da Silva, L. R. D.; Goes, J. C.; Jardim, P. M.; et al. Sintering of Nanoparticles of α-Fe_2O_3 Using Gelatin. *Journal of Non-Crystalline Solids* **2007,** *353,* 1091-1094.

[12] Campá, J.; Gutiérrez-Puebla, E.; Monge, A.; Rasines, I.; Ruíz-Valero, C. $Sr_9Ni_{6.64}O_{21}$: A New Member (n = 2) of the Perovskite-Related $A_{3n+3}A_n'B_{3+n}O_{9+6n}$ Family. *J. Solid State Chem.* **1996,** *126,* 27-32.